Deposition Characteristics of Ti-Si-N Films Reactively Sputtered from Various Targets in a N_2/Ar Gas Mixture

W.H. LEE,[1,3] S.K. PARK,[1] B.J. KANG,[1] P.J. REUCROFT,[2] and J.G. LEE[1]

1.—Kookmin University, School of Metallurgical and Materials Engineering, 861-1, Joengneung-Dong, Sungbuk-Gu, Seoul 136-702, Korea. 2.—University of Kentucky, Department of Chemical and Materials Engineering, University of Lexington, KY 40506. 3.—e-mail: whlee9@kmu.kookmin.ac.kr

The deposition characteristics of Ti-Si-N films obtained by using RF reactive sputtering of various targets in N_2/Ar gas mixtures have been investigated. The dependence of film growth rate and stoichiometry on both the Ti/Si ratio of the target and the N_2 flow rate were found to be due to the different nitridation rates of Ti and Si, resulting in different sputter yields of titanium and silicon nitrides. XPS results showed that an increase in nitrogen content of the Ti-Si-N films leads to the formation of amorphous Si_3N_4 bonding, which produces an increase in resistivity. Lowering the Si content in the deposited Ti-Si-N films favors the formation of crystalline TiN, even at low N_2 flow rates, and leads to a lower resistivity. A film growth mechanism, expressed in terms of the nitrogen surface coverage on the target, was proposed.

Key words: Metallization, diffusion barrier, titanium nitride, RF sputtering, XPS

INTRODUCTION

Copper has received considerable attention as a potential interconnect material in advanced metallization technology because it intrinsically exhibits superior electromigration resistance and lower resistivity compared to conventional Al metallization.[1–6] However, important technical problems that need to be addressed include: passivation of the exposed Cu surface against oxidation, adhesion of Cu to SiO_2, development of a process for patterning Cu, and the high diffusivity of Cu in Si and SiO_2.[7–9] A number of approaches have been explored to address these problems, such as the development of Cu passivation methods and diffusion barrier materials.[10–23]

The study of diffusion barrier materials for their application in ULSI has been more critical. TiN has been widely used as a diffusion barrier material.[24,25] Especially, ternary diffusion barriers of the TM-Si-N (TM = Ta, Mo, or W) type have shown superior performance in Cu metallization.[26–30] There have also been intensive studies on Ti-Si-N films using various deposition and annealing methods.[31–35] It has been shown that the diffusion capability and resistivity variation of this film are mostly influenced by the film composition. Therefore, systematic studies of the deposition characteristics of Ti-Si-N films are necessary. However, there have not been any studies on the deposition characteristics of Ti-Si-N films deposited by radio frequency magnetron sputtering in terms of the effects of target composition and N_2 flow rate in a N_2/Ar ambient.

In this paper, various stoichiometric Ti-Si-N films have been deposited from 4 different targets. Experimental studies were designed to alter the various properties of the Ti-Si-N films by employing reactive radio frequency (RF) sputtering methods. The effects of target composition and N_2 flow rate on the film growth rate, resistivity, density and compressive stress have been investigated. The deposition mechanism was systematically studied and the film growth rate was expressed in terms of the nitrogen surface coverage on the target.

(Received June 12, 2000; accepted October 26, 2000)

EXPERIMENTAL

Ti-Si-N films were deposited in a Ar/N_2 gas atmosphere on to a p-type (100) Si wafer by using (RF) magnetron reactive sputtering from 4 different targets (a: a 2″-$TiSi_2$ target, b: a Si chip (2 cm × 2 cm) on a 2″-Ti target, c: a Ti chip (2 cm × 2 cm) on a 2″-$TiSi_2$

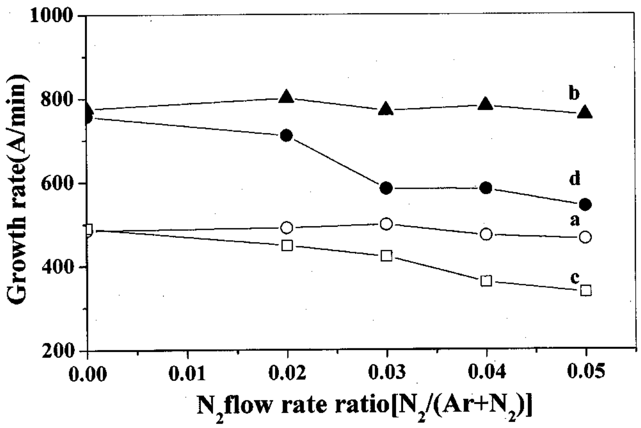

Fig. 1. Growth rate of Ti-Si-N films deposited from four different targets as a function of N_2 flow rate (a) $TiSi_2$ target, (b) Si chip (2 cm × 2 cm) on a Ti target, (c) Ti chip (2 cm × 2 cm) on a $TiSi_2$ target, and (d) Si chip (1 cm × 1 cm) on a Ti target.

target, and d: a Si chip(1 cm × 1 cm) on a 2″-Ti target.) In all deposition processes, the distance between the substrate and the target, the RF power, and the substrate temperature were fixed at 40 mm, 180 W, and ambient temperature, respectively. The working pressure was kept at 2 mtorr. Various stoichiometric Ti-Si-N films were obtained by varying the N_2 flow rate during sputtering.

Quantitative analysis of the stoichiometric composition of the Ti-Si-N films was conducted using Rutherford backscattering spectroscopy (RBS). Film resistivity was measured by a four point probe method. X-ray photoelectron spectroscopy (XPS) was used to analyze the chemical bonding state of the Ti-Si-N films. Finally, residual stress of the films was obtained by using a surface profilometer.

RESULTS AND DISCUSSION

Figure 1 shows the growth rate of Ti-Si-N films deposited from the four different targets at various N_2 flow rates. The growth rate strongly depended on the target composition; a lower growth rate was obtained by using a $TiSi_2$ target compared to a Ti target. The lower growth rate can be attributed to the low sputter yield resulting from the higher Ti-Si bonding strength in the $TiSi_2$ target. As the N_2 flow rate increased, the growth rate decreased when Ti rich targets were used (a and d). The dependence of film growth rate on N_2 flow rate when using the 4 different targets appears to be due to different nitridation rates of Ti and Si, leading to different sputter yields. To elucidate the different sputter yields, the variation of growth rate with increased N_2 flow rate when using pure Si and pure Ti targets was investigated. Figure 2 shows the growth rates of TiN and SiN_x films deposited at various N_2 flow rates in N_2/(Ar+N_2). It can clearly be seen that similar deposition rates were obtained regardless of the targets used when only Ar gas was employed, whereas the growth rate of TiN significantly decreased as the N_2 flow increased. Tsai et al., reported that the dependence of the TiN growth rate on the N_2 flow rate could be attributed to different

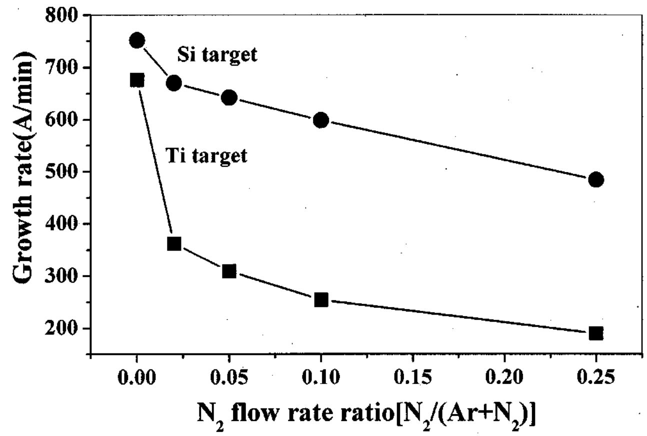

Fig. 2. Growth rate of TiN and SiN_x films deposited from a Ti target and a Si target as a function of N_2 flow rate.

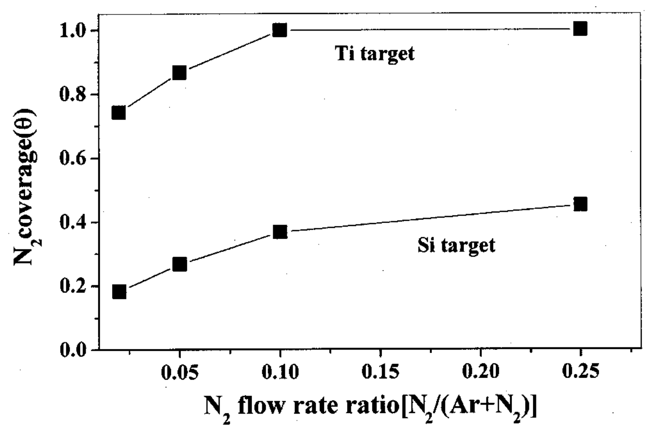

Fig. 3. Nitrogen coverage on a Ti target and a Si target obtained as a function of N_2 flow rate.

nitrogen coverages on the Ti target.[36] Based on their mathematical simulation, growth rate Eqs. 1 and 2 for the deposition of TiN and SiN_x films are proposed:

$$R_{TiN} = S\left[F_{TiN} Y_{TiN} \theta_N^{Ti} + F_{Ti} T_{Ti}\left(1-\theta_N^{Ti}\right)\right] \quad (1)$$

$$R_{SiNx} = S\left[F_{SiNx} Y_{SiNx} \theta_N^{Si} + F_{Si} Y_{Si}\left(1-\theta_N^{Si}\right)\right] \quad (2)$$

R is the growth rate and S is the Ar^+ flux applied to the target. Y is the sputter yield of deposited film, where Y_{Ti}, Y_{Si} = 0.3 and Y_{TiN}, Y_{SiNx} = 0.1 with a sputter power of 300 V. θ_N is the surface coverage of nitrogen atoms on the target. F represents the thickness increase produced by deposition of a single atom or molecule. For example, $F_{TiN} = 1.98 \times 10^{-23}$ cm^3/molecule, $F_{Ti} = 1.76 \times 10^{-23}$ cm^3/atom, $F_{SiNx} = 2.49 \times 10^{-23}$ cm^3/molecule, and $F_{Si} = 1.99 \times 10^{-23}$ cm^3/atom. The nitrogen content of the deposited Ti-Si-N films was determined by RBS and the values of θ_N were obtained from Eqs. 1 and 2. S_{TiN} and $S_{SiN,}$ using only Ar gas were 2.133×10^{16} ions/cm^2-s and 2.124×10^{16} ions/cm^2-s, respectively. Figure 3 shows the resulting values of nitrogen coverage on the Ti and Si targets at various N_2 flow rates. In the case of a pure Ti target, the surface coverage (θ_N) was about 70% even with a 2% N_2 flow rate. Furthermore, the surface coverage was fully saturated at a 10% N_2

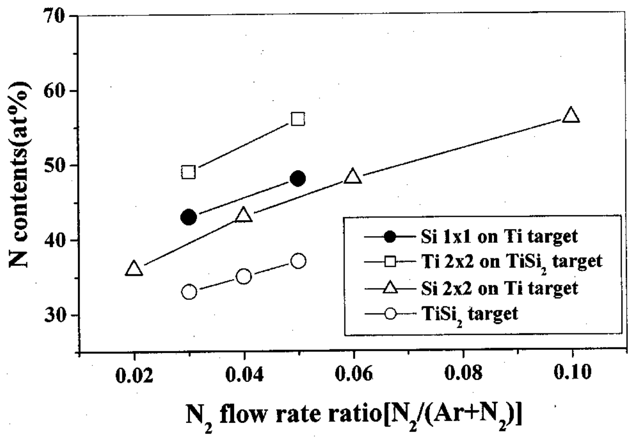

Fig. 4. Nitrogen content of TiN and SiN_x films deposited from four different targets as a function of N_2 flow rate.

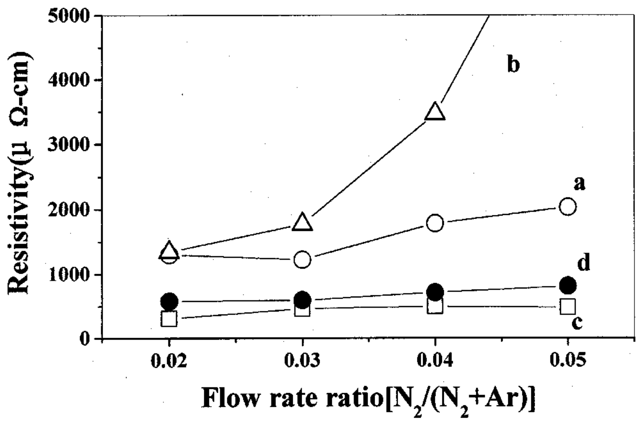

Fig. 5. Resistivity of Ti-Si-N films deposited from four different targets as a function of N_2 flow rate.

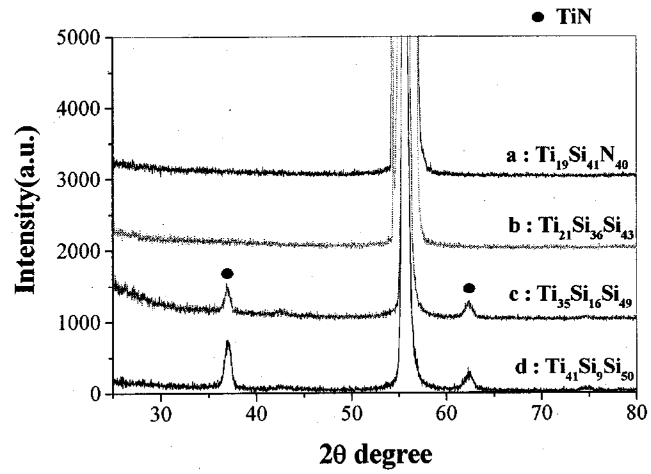

Fig. 6. XRD patterns of Ti-Si-N films deposited from four different targets at a N_2 flow rate ratio of 0.04.

flow rate. On the other hand, only 20% surface coverage of N_2 on Si was obtained with a 2% N_2 flow rate. As the flow rate increased, the surface coverage of nitrogen on the Si target continued to increase. It can be concluded that the growth rate of Ti-Si-N films strongly depends on the Ti/Si ratio of the target. Therefore, higher deposition rates of Ti-Si-N films were obtained by using a target with a higher Si/Ti ratio. In this case, the growth rate shows a relatively constant value even with increased N_2 flow. Figure 4 shows the N content variation of Ti-Si-N films deposited using four different targets at various N_2 flow rates. With all the targets, the nitrogen content increased with increased N_2 flow. It was confirmed that a higher nitrogen content of the deposited films using targets with higher Ti/Si ratios can be obtained at the same N_2 flow rate.

Figure 5 shows the resistivity of Ti-Si-N films deposited using four different targets at various N_2 flow rates. It can be seen that films deposited using targets (c) and (d), which have relatively high Ti/Si ratios, showed lower resistivity. The resistivity appears to be constant even with increasing N_2 flow rate, as described previously. Lower resistivity can also be due to the formation of TiN in the Ti-Si-N film. On the other hand, the Ti-Si-N films deposited using targets (a) and (b), which have relatively high Si/Ti ratios, showed high resistivity. As the N_2 flow rate increased, the resistivity continued to increase. This is because the nitridation of Si proceeds further, as seen in Fig. 3. It can thus be concluded that the increased resistivity is due to the formation of Si_3N_4 in the Ti-Si-N films. XRD results confirmed the formation of TiN in the Ti-Si-N films, as shown in Fig. 6. The x-ray patterns of $Ti_{41}Si_9N_{50}$ and $Ti_{35}Si_{16}N_{49}$ films deposited from targets (c) and (d), respectively, at a flow rate ratio of 0.04, show diffraction peaks that can be assigned to crystalline TiN. $Ti_{19}Si_{41}N_{40}$ and $Ti_{21}Si_{36}N_{43}$ films deposited from targets (a) and (b), respectively, showed an amorphous structure. Their higher resistivity is thus most likely due to the formation of amorphous Si_3N_4.

Figure 7 shows XPS narrow scan spectra of (a) Ti 2p, (b) Si 2p, and (c) N 1s from $Ti_{21}Si_{36}N_{43}$ and $Ti_{41}Si_9N_{50}$ films. XPS peaks of TiN are also included for comparison. From the Ti 2p narrow scan spectra of the $Ti_{41}Si_9N_{50}$ film, Ti was mainly in the form of TiN, in good agreement with the XRD results. In the case of the $Ti_{21}Si_{36}N_{43}$ film, typical peak broadening and relatively weak intensity of the Ti $2p_{3/2}$ peak were observed, suggesting the existence of small amounts of TiN and other Ti based compounds such as TiSi. From the Si 2p narrow scan spectra, the chemical bonding state of Si in the $Ti_{21}Si_{36}N_{43}$ film was mainly in the form of Si_3N_4 with relatively small amounts of $TiSi_x$ or unreacted Si. This result is confirmed by the N 1s spectra (Fig. 7c). It thus appears that Si_3N_4 bonding predominates in $Ti_{21}Si_{36}N_{43}$ films and incorporation of additional nitrogen produces Si_3N_4 and a small amount of TiN bonding. On the other hand, the amount of Si in the $Ti_{41}Si_9N_{50}$ film in the form of Si_3N_4 appeared to be very small. From the N 1s narrow scan spectra, the chemical bonding state of N in the $Ti_{21}Si_{36}N_{43}$ film was mainly in the form of Si_3N_4 with relatively small amounts of TiN, while that of N in the $Ti_{41}Si_9N_{50}$ film was mainly in the form of TiN with relatively small amounts of Si_3N_4. From the XPS results, it can be concluded that the $Ti_{21}Si_{36}N_{43}$ film is mainly composed of Si_3N_4, unreacted Si (or $TiSi_x$), and TiN while the

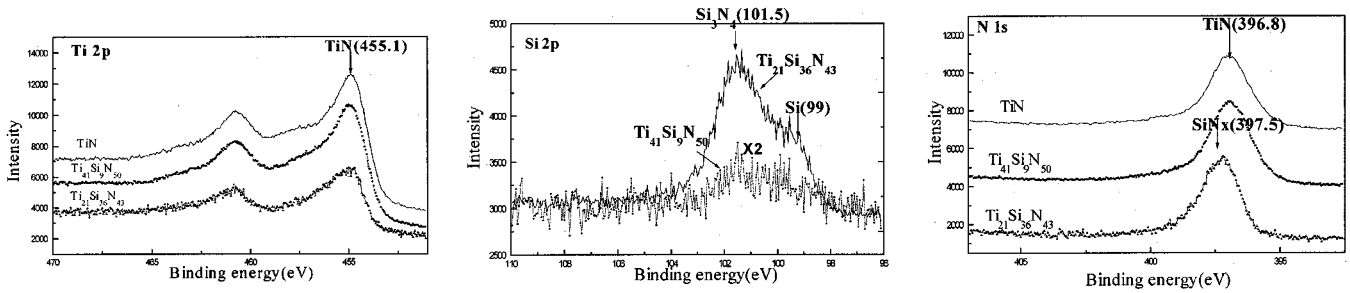

a b c

Fig. 7. XPS narrow scan spectra of (a) Ti 2p, (b) Si 2p, and (c) N 1s from $Ti_{41}Si_9N_{50}$ and $Ti_{21}Si_{36}N_{43}$ films.

$Ti_{41}Si_9N_{50}$ film is mainly composed of TiN with small amounts of Si_3N_4. It can also be concluded that the low resistivity of Ti-Si-N films deposited over wide N_2 flow rate range can be attributed to the existence of crystalline TiN. The increased resistivity of Ti-Si-N films with increased N_2 flow rate can be attributed to the further formation of amorphous Si_3N_4. Figure 8a and b show the density and compressive stress of various stoichiometric Ti-Si-N films obtained by manipulating the targets and N_2 flow rates, respectively. It can be seen that the film density increases with increased film nitrogen content and the compressive stress also increases. The current experimental results suggest that the diffusion barrier capability of the Ti-Si-N films can be superior due to increased film density. However, significantly higher nitrogen content over 55% can degrade the diffusion barrier characteristics due to higher compressive stresses in the films.

In conclusion, various stoichiometric Ti-Si-N films can be obtained as candidates for advanced metallization schemes by manipulating the Ti/Si ratio of the target and the N_2 flow rate in a reactive RF magnetron sputtering system.

SUMMARY

The deposition characteristics of Ti-Si-N films obtained by using RF reactive sputtering of targets with various Ti/Si ratios in a $N_2/(Ar + N_2)$ gas mixture have been investigated. The dependence of film growth rate and stoichiometry on the Ti/Si ratio of the target and the N_2 flow rate were governed by the different nitridation rates of Ti and Si, resulting in different sputter yields of titanium and silicon nitrides. The chemical bonding state of Si in the Ti-Si-N film, which contained a higher Si content, was in the form of amorphous Si_3N_4, producing increased film resistivity with increased N_2 flow rate. Lowering the Si content in the deposited Ti-Si-N film favored the formation of crystalline TiN even at low N_2 flow rates, and leads to low film resistivity. In addition, increasing the N content led to Ti-Si-N films having a higher density and compressive stress, suggesting that the N content in the films appears to be one of the most important factors affecting the diffusion barrier characteristics. In the current work, it was concluded that the various stoichiometric Ti-Si-N films for desired optimum properties can be controlled by manipulating the Ti/Si ratio of the target and the N_2 flow rate.

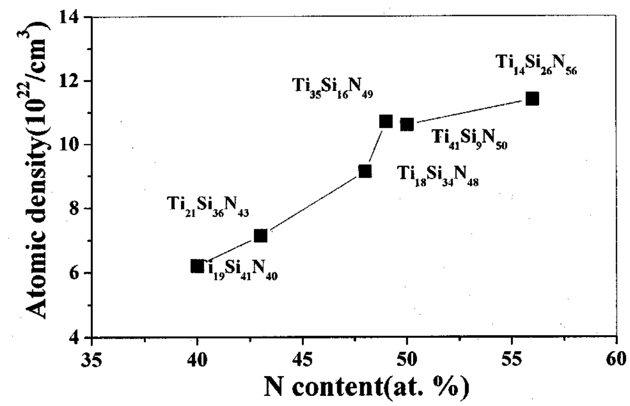

a

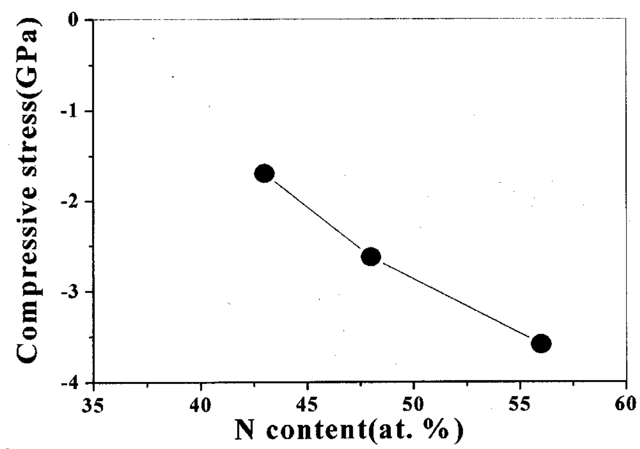

b

Fig. 8. (a) The density and (b) compressive stress of various stoichiometric Ti-Si-N films as a function of N content.

ACKNOWLEDGEMENTS

This work was supported by the Brain Korea 21 Project. This work has also been supported in part from the G-7 through the Korean Ministry of Commerce, Industry and Energy and the Korean Ministry of Science and Technology.

REFERENCES

1. N. Awaya and Y. Arita, *J. Electron. Mater.* 21, 959 (1992).
2. A. Jain, T. Kodas, R. Jairath, and M.J. Hampden-Smith, *J. Vac. Sci. & Technol.* B11, 2107 (1993).
3. J. Lin and M. Chen, *Jpn. J. Appl. Phys.* 38, 4863 (1999).
4. S.P. Murarka and S. Hymes, *Solid State Mater. Sci.* 20, 87 (1995).

5. Y.J. Park, V.K. Andleigh, and C.V. Thompson, *J. Appl. Phys*. 85(7), 3546 (1999).
6. C. Whitman, M.M. Moslehi, A. Paranjpe, L. Velo, and T. Omstead, *J. Vac. Sci. & Technol*. A 17, 1893 (1999).
7. R. Liu, C.S. Pai, and E. Martinez, *Solid State Electr*. 43, 1003 (1999).
8. X.W. Lin and D. Pramanlk, *Solid State Technol.* October, 63 (1998).
9. W.C. Roh and D.J. Jung, *Jpn. J. Appl. Phys*. 37, 406 (1998).
10. P.J. Ding, W. Wang, W.A. Lanford, S. Hymes, and S.P. Murarka, *Appl. Phys. Lett*. 65, 1778 (1994).
11. H. Itow, Y. Nakasaki, G. Minamihaba, K. Suguro, and H. Okano, *Appl. Phys. Lett*. 63, 934 (1993).
12. W.A. Lanford, P.J. Ding, W. Wang, S. Hymes, and S.P. Murarka, *Thin Solid Films* 262, 234 (1995).
13. P.J. Ding, W.A. Lanford, S. Hymes, and S.P. Murarka, *J. Appl. Phys*. 74, 1331 (1993).
14. S. Hymes, S.P. Murarka, S. Shepard, and W.A. Lanford, *J. Appl. Phys*. 71, 4623 (1992).
15. J. Li, J.W. Mayer, and E.G. Colgan, *J. Appl. Phys*. 70, 2820 (1991).
16. Y. Wang and T.L. Alford, *Appl. Phys. Lett*. 74, 52 (1999).
17. Y.T. Kim, C.H. Jun, and D.Y. Kim, *J. Electron. Mater*. 28, 369 (1999).
18. S.H. Lee, D.J. Kim, S.H. Yang, J.W. Park, K.H. Oh, Y.T. Kim, J.Y. Kim, G.Y. Yeom, and J.W. Park, *J. Appl. Phys.* 85, 473 (1999).
19. H.K. Shin, H.J. Shin, J.G. Lee, S.W. Kang, and B.T. Ahan, *Chem. Mater*. 9(1), 76 (1997).
20. D.H. Kim, G.T. Kim, S.K. Kim, J.W. Park, and G.G. Lee, *J. Vac. Sci. Technol*. B17, 2197 (1999).
21. J.G. Lee, H.L. Cho, E.G. Lee, J.Y. Lee, K.B. Kim, and J.M. Lee, *J. Kor. Phys. Soc*. 35, 65 (1999).
22. W.H. Lee, H.L. Cho, B.S. Cho, J.Y. Kim, Y-S. Kim, W.G. Jung, H. Kwon, J.H. Lee, P.J. Reucroft, C.M. Lee, and J.G. Lee, *J. Electrochem. Soc*. 147, 3066 (2000).
23. W.H. Lee, H.L. Cho, B.S. Cho, J.Y. Kim, W.J. Nam, Y-S. Kim, W.G. Jung, H. Kwon, J.H. Lee, J.G. Lee, P.J. Reucroft, C.M. Lee, and E.G. Lee, *Appl. Phys. Lett.* 77, 2192 (2000).
24. N. Cheung, H. von Seefeld, and M.A. Nicolet, *Thin Film Interface and Interconnections,* ed. J.E. Boglin and J.M. Poate (Princeton, NJ: The Electrochem. Soc., Inc, 1990), p. 323.
25. S.Q. Wang, I. Raaijmakens, B.J. Burrow, S. Suthar, and S. Redkar, *J. Appl. Phys*. 68, 5176 (1990).
26. H. Sugahara and J. Nagano, *Appl. Surf. Sci*. 41/42, 207 (1989).
27. J.S. Reid, E. Kolawa, C.M. Garland, M.A. Nicolet, F. Cardone, D. Gupta, and R.P. Ruiz, *J. Appl. Phys*. 79, 1109 (1996).
28. E. Kolawa, J.M. Molarius, C.W. Nieh, and M.A. Nicolet, *J. Vac. Sci. Technol*. A8, 3006 (1990).
29. E. Kolawa, J.S. Chen, J.S. Reid, P.J. Pokela, and M.A. Nicolet, *J. Appl. Phys*. 70, 1369 (1991).
30. J.S. Reid, E. Kolawa, R.P. Ruiz, and M.A. Nicolet, *Thin Solid Films* 236, 319 (1993).
31. M. Diserens, J. Patscheider, and F. Levy, *Surf. Coatings Technol*. 108/109, 241 (1998).
32. F. Vaz, L. Rebouta, B. Almeida, P. Goudeau, J. Pacaud, J.P. Riviere, and J. Bess e Sousa, *Surf. Coatings Technol*. 120/121, 166 (1999).
33. J.S. Min, H.S. Park, and S.W. Kang, *Appl. Phys. Lett*. 75(11), 1521 (1999).
34. X. Sun, J.S. Reid, E. Kolawa, and M.A. Nicolet, *J. Appl. Phys*., 81(2), 656 (1997).
35. J.S. Park, D.K. Sohn, B.H. Lee, J.U. Bae, J.S. Byun, and J.W. Park, *J. Electrochem. Soc*. 146, 1579 (1999).
36. W. Tsai, J. Fair, and D. Hodul, *J. Electrochem. Soc*. 139, 2004 (1992).